ChemistrySelect

Research Article
doi.org/10.1002/slct.202300277

Chemistry Europe
European Chemical
Societies Publishing

www.chemistryselect.org

Discovery of Potential KRAS-SOS1 Inhibitors from South African Natural Compounds: An *In silico* Approach

Abdul Rashid Issahaku,[a] Elliasu Y. Salifu,[a] Clement Agoni,[a] Mohammed Issa Alahmdi,[b] Nader E Abo-Dya,[c] Mahmoud E. S. Soliman,[a] Mithun Rudrapal,*[d] and Naresh Podila[d]

For decades the direct targeting of KRAS as a driver of non-small cell lung cancer, colorectal and pancreatic cancers as well as the inhibition of the RAF-MEK-ERK pathway has shown little success due to feedback networks that keep the pathway in control. Inhibiting SOS1, a KRAS activator, has therefore become a promising escape route to treating KRAS-driven cancers. The search for SOS1 inhibitors has since gained momentum although no drug has been approved yet. Owing to the time-consuming and difficult processes that characterize the discovery and approval of drugs, natural products have become useful in addressing the unmet medical needs. In this study we employed computational techniques to screen South African natural products for inhibitors with the potential to inhibit SOS1-KRAS activation. In this study, eight natural compounds, from plants and marine life, possessing antineo-plastic activities with good docking and ADMET properties were identified. These compounds, viz., SANCDB00219, SANCDB0290, SANCDB00369, SANCDB00416, SANCDB00421, SANCDB00749, SANCDB00957 and SANCDB001124 exhibited favorable total free binding energies in complex with SOS1-KRAS characterized by conventional and carbon hydrogen bonds, van der Waals, pi-alkyl and pi-sigma interactions with the binding site residues. It was further revealed that these compounds induced conformational stability on the structural architecture of SOS1-KRAS, and decreased the structural flexibility of its individual C-α atoms as a mechanism of inhibition. Upon experimental validation, these compounds from a natural origin could serve as lead identification of small molecules to address SOS1-KRAS associated diseases.

Introduction

For decades now the RAS family of GTPases (KRAS, NRAS and HRAS) have been identified as major oncogenes in cancer developments among humans and is estimated to account for up to 20 to 30% of cancers.[1–3] This family of proteins circles between the active and inactive states thus serving as molecular switches in cell proliferation, signaling and survival. RAS proteins become active when bound to GTP and inactive when bound to GDP.[4] These switching 'ON' and 'OFF' states are tightly controlled by multi-domain proteins; guanine nucleotide exchange factors (GEFs) and GTPase-activating proteins (GAPs) respectively.[3] In the deactivation process, GAP down-regulates the active RAS by catalyzing the weak intrinsic GTPase activity by up to 5 folds magnitude.[5] However, in oncogenic RAS mutants, the deactivation activity of GAP is significantly reduced or impaired leading to constant activation which conditions oncogenic RAS signaling.[6] As reported, important RAS signaling pathways such as RAS-RAF-MEK-ERK and RAS-PI3 K-PDK1-AKT become uncontrollable.[7] With difficulty in direct therapeutic targeting of RAS due to high picomolar affinity of GTP to the binding site, coupled with its abundance in the cytosol and lack of deep pockets to accommodate small molecules, drug developers redirected their focus to (1) covalently targeting Cys12 of the oncogenic mutant KRAS^{G12C}, (2) RAS-effector interactions to sever downstream signaling, and (3) inhibition RAS-GEF interactions to prevent rebounding of GTP.[1,8,9] Strenuous efforts resulted in some success in the first two strategies wherein discovered small molecules are at various stages of clinical trials[10–14], however this success is limited to a small number of clients where the cancer is derived by KRAS particularly KRAS^{G12C} mutants. Targeting RAS-GEF interactions, though very challenging could results in inhibiting all the RAS isoforms including their mutant forms. As such, every arsenal is being deployed to break through this critical protein-protein interaction (PPI). PPIs are estimated to engage in approximately 500,000 interactions in the human system and are therefore critical for essential biological processes[15].

[a] Dr. A. R. Issahaku, Dr. E. Y. Salifu, Dr. C. Agoni, Dr. M. E. S. Soliman
Molecular Bio-computation and Drug Design Laboratory
School of Health Sciences
Westville Campus,
University of KwaZulu-Natal
Durban 4001, South Africa

[b] Dr. M. I. Alahmdi
Faculty of Science
Department of Chemistry
University of Tabuk
Tabuk 7149, Saudi Arabia

[c] Dr. N. E Abo-Dya
Faculty of Pharmacy
Department of Pharmaceutical Chemistry
University of Tabuk
Tabuk 71491, Saudi Arabia

[d] Dr. M. Rudrapal, Dr. N. Podila
Department of Pharmaceutical Sciences
School of Biotechnology and Pharmaceutical Sciences
Vignan's Foundation for Science
Technology & Research (Deemed to be University)
Guntur 522213, India
E-mail: rsmrpal@gmail.com

Supporting information for this article is available on the WWW under https://doi.org/10.1002/slct.202300277

ChemistrySelect

Research Article
doi.org/10.1002/slct.202300277

Chemistry
Europe
European Chemical
Societies Publishing

The Son of Sevenless(SOS1 and 2) proteins, SOS1 and SOS2 are the most studied RAS-GEF protein-protein interaction proteins which are reported to engage in distinct PPIs with RAS[16–18] with reports suggesting only SOS1 is susceptible to allosteric inhibition[19] (Figure 1). Several attempts has therefore been made to inhibit RAS-SOS1 interaction through peptides and small molecules which resulted in moderate affinity[20–23] and undesired SOS1activation resulting in biphasic modulation of RAS signaling through negative feedback on SOS1.[24] Nonetheless, the search for RAS inhibitors continuous unabated.

Owing to the expensive and time-consuming processes involved in drug discovery and development, which normally take several years to get a drug to the clinic,[25–27] drug repurposing has become very useful in addressing the unmet medical needs of patients.[28,29] This provides an efficient strategy and escape route in medicinal chemistry to avoid preclinical and optimization shortcomings as well as adverse
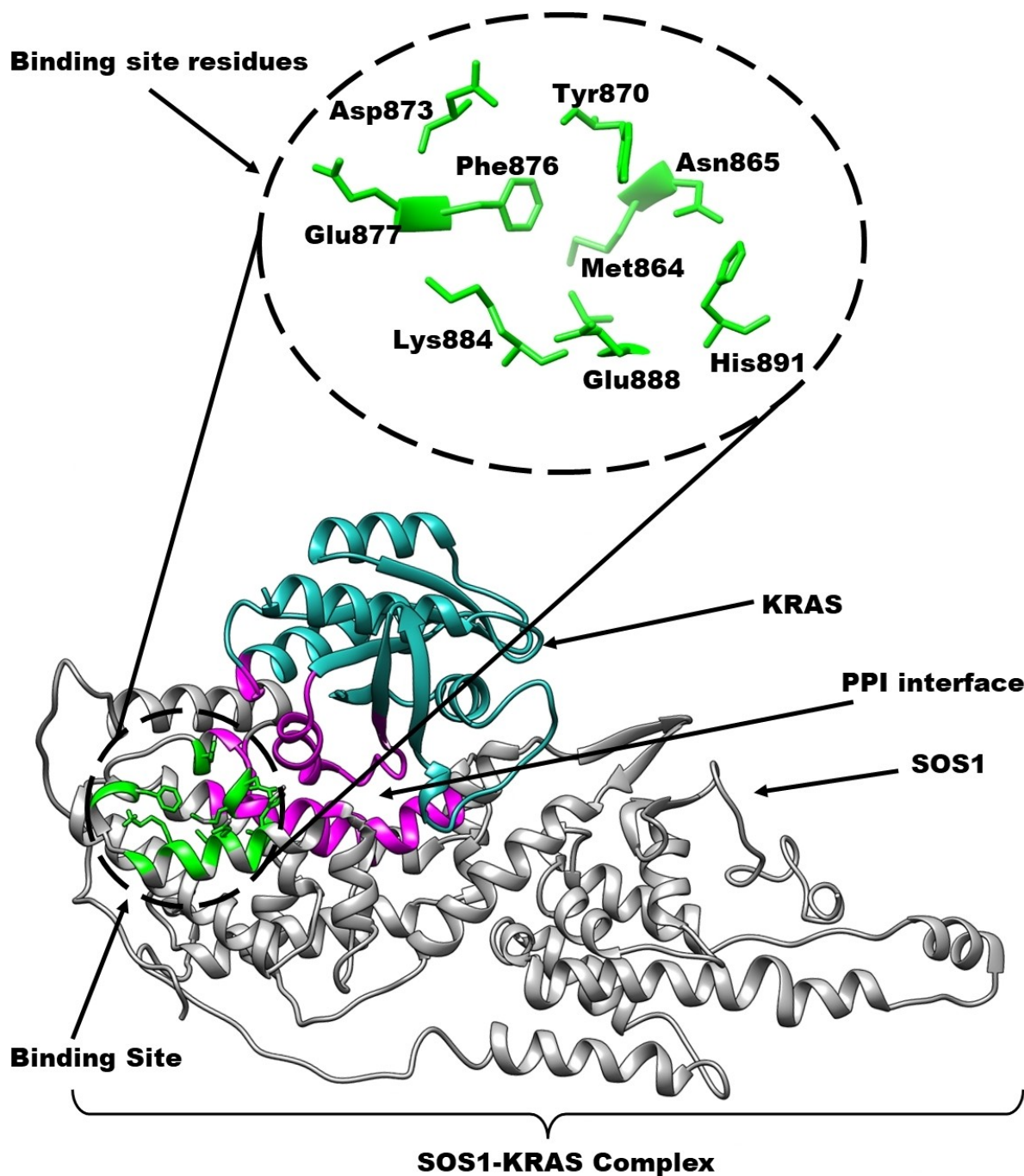

Figure 1. Structure of Son of Seveless 1 (SOS1-KRAS)-KRAS complex showing the allosteric binding site (green) on the SOS1-KRAS protein (dark grey), the protein-protein interaction interface (magenta), and the KRAS protein (light sea green). Insert shows the binding site residues.

ChemistrySelect

Research Article
doi.org/10.1002/slct.202300277

Chemistry Europe
European Chemical
Societies Publishing

toxicological profiles.[30] Though most repurposing strategy rely on synthesized compounds, natural compounds equally provide significant opportunities.[31] Characterized by unique and favorable properties with notable structural diversity and high number of pharmacological activities,[32] natural products present drug rediscovery opportunities wherein therapeutic activities initially unrelated to their original biological space could be utilized.[33]

In this study, we utilized South Africa's natural compounds database together with computational techniques to identify potential SOS1 inhibitors that would be useful in addressing the unmet medical needs of patients suffering from RAS oncogenic signaling pathway involving SOS1. This database was chosen because it contains novel scaffolds that have not been fully exploited for their therapeutic potentials.

Results and discussion

The three-dimensional (3D) X-ray structures of the SOS1-KRAS (PDB IDs: 7KFZ, 6EPN and 6EPP) were retrieved from the protein data bank. The 7KFZ structure contained two KRAS chains that binds to the allosteric and active site. The chain bound to the allosteric site was deleted to create similarity between the structures. Ramachandran plots used for validating the structures showed 99.453%, 98.107% and 98.367% of amino acids for 7KFZ, 6EPP and 6EPN, respectively were in the favored region. Qualitative Model Energy Analysis (QMEAN) which predicts the quality of a crystal structure by its QMEAN Z-score and QMEAN4 global score was also carried out. The analysis using Protein Structure Analysis (ProSA) tool gave an overall model quality with Z-score of −7.72 (7KFZ), −7.48 (6EPN) and −7.28 (6EPP) indicating the structures are of high quality. The QMEAN4 global score was 0.84 (7KFZ) and 0.86 for both 6EPN and 6EPP which fell within the desired range of 0 to 1. The graphs showing the validation of SOS1-KRAS protein structures used for docking and MD simulation are presented in the Supplementary Figure S1.

Structure-based virtual screening

Natural compounds and their peculiar scaffolds are an important start point for drug discovery.[34] The known inhibitors showed binding affinities of −8.5 kcal/mol, −8.3 kcal/mol, −7.9 kcal/mol and −7.6 kcal/mol for the inhibitors Compound 9, BAY-293, BI-3406 and BI-68BS, respectively. The docking scores presented by these inhibitors then served as a basis to select compounds that exhibited similar binding affinities. The interplay of analyses involving the binding affinities, the pharmacokinetics, and the compounds' activities against cancers in which SOS1-KRAS over expression is implicated resulted in the identification of the compounds shown in Table 1. The docking score for natural compounds and known inhibitors are detailed in Supplementary Table S1 and Table S2.

Hit compound interactions within the binding pocket

The type of interactions a compound engages in within the binding pocket of a target protein underscores its therapeutic influence on the protein.[35] After the selection of the compounds, we endeavored to ascertain the interactions that characterize the binding process. The known inhibitors were observed to engage in varied interactions involving conventional and carbon hydrogen bonds, van der Waals and pi-interaction as depicted in Figure 2. The interaction types between the inhibitors and the site residues varied depending on the inhibitors' functional groups. Assessing the interaction profile of the selected compounds showed similar interaction types as observed in Figure 2. The selected compounds interacted with residues VAL861, MET864, ASN865, TYR870, ASP873, PHE876, GLU877, LYS884, LEU887, GLU888, ALA890, HIS891, GLU892, and GLU895.
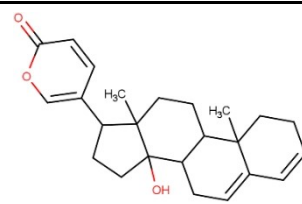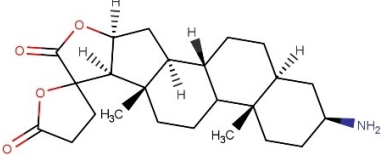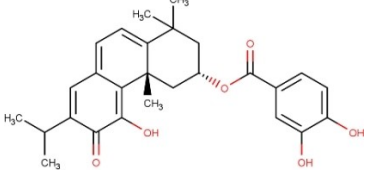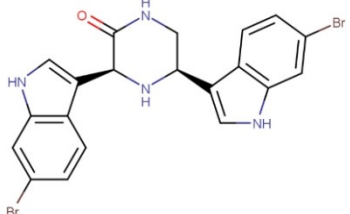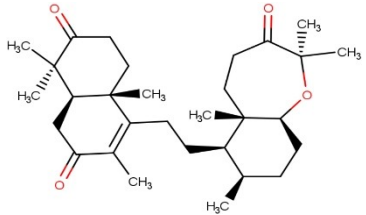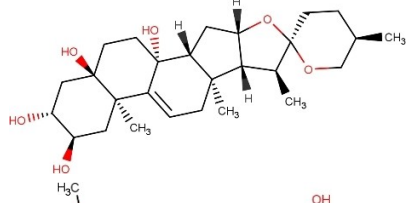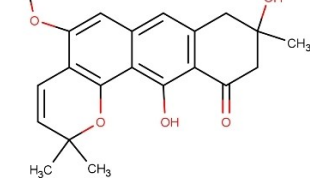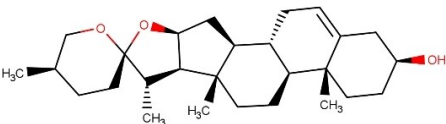
Binding energy landscape of selected compounds

The MMPBSA method of estimating the total free binding energies of the selected compounds were carried out and tabulated in Table 2. The results presented similar total free binding energies of −36.32 ± 4.23 kcal/mol, −32.42 ± 4.67 kcal/mol, −42.09 ± 3.54 kcal/mol, −32.23 ± 4.54 kcal/mol, −30.25 ± 3.41 kcal/mol, −30.89 ± 4.56 kcal/mol, −32.21 ± 4.26 kcal/mol, and −35.11 ± 5.98 kcal/mol for SANCDB00219, SANCDB00290, SANCDB00369, SANCDB00416, SANCDB00421, SANCDB00749, SANCDB00957 and SANCDB1124 respectively. As observed SANCDB00369 presented the highest total free binding energy whiles while SANCDB00290 presented the least. The energies presented by these compounds suggests the spontaneity, permeation and a measure of the reaction kinetics that characterize their complex formation with the SOS1-KRAS protein.[36] It was also observed that van der Waals, electrostatic and the gas phase terms contribute favourably to the bind of the compounds whiles the solvation term opposed them.

General information of identified hit compounds

The 14β-Hydroxybufa-3,5,20,22-tetraenolide compound (SANCDB ID: SANC00219) is a bufadienolide/steroid that is extracted from *Urginea epigea*and known to possess vascular myorelaxing activity acting partly through the activation of soluble guanylyl cyclase.[37,38] Clionamine D with SANCDB ID, SANC00290, is an aminosteroid extracted from marine life (*Cliona celata*), an orange excavating boring sponge and used as an autophagy-modulator[74] Parviflorone F compound with SANCDB ID; SANC00369 is a compound that has been used as an antimalaria drug. It is a terpenoid/diterpene extracted from the leaves of *Plectranthus ecklonii*.[39] Cis-3,4-dihydrohamacanthin b is an alkaloid/indole compound (SANCDB ID: SANC00416) which is derived from *Topsentia parchastrelloides.*This compound has been used as an antibacterial agent and has proved effective in the inhibition of pyruvate kinase in methicillin-resistant *Staphylococcus aureus*.[40] Sodwanone R (SANCDB ID: SANC00421) is an isoprenoid isolated from marine

ChemistrySelect

Research Article
doi.org/10.1002/slct.202300277

Chemistry Europe
European Chemical
Societies Publishing

Comp. name	SANCDB ID	Docking score(kcal/mol)	2D structure
Table 1. Docking score of top favorable compounds against SOS1-KRAS with their 2D structures.			
14β-Hydroxybufa-3,5,20,22-tetraenolide	00219	−9.1	
Clionamine D	00290	−9.6	
Parviflorone F	00369	−9.1	
Cis-3,4-dihydrohamacanthin b	00416	−8.9	
Sodwanone R	00421	−8.7	
9(11)-Dehydroagapanthagenin	00749	−8.7	
Vismione B	00957	−8.8	
Diosgenin	1124	−8.9	

sponges of the family axinellidae. The use of this compound is not yet known.[41] 9(11)-Dehydroagapanthagenin with SANCDB ID: SANC00749 is a spirostan sapogenin isolated from *Agapanthus africanus* whose medical used is not yet known.[42]

Vismione B is a cytotoxic naphthopyrans compound extracted from the plant *Vismia baccifera*(SANCDB ID: SANC00957), whose medical use is not yet known.[43] Diosgenin is a phenol lipids compound (SANCDB ID: SANC1124) with cytotoxic activities
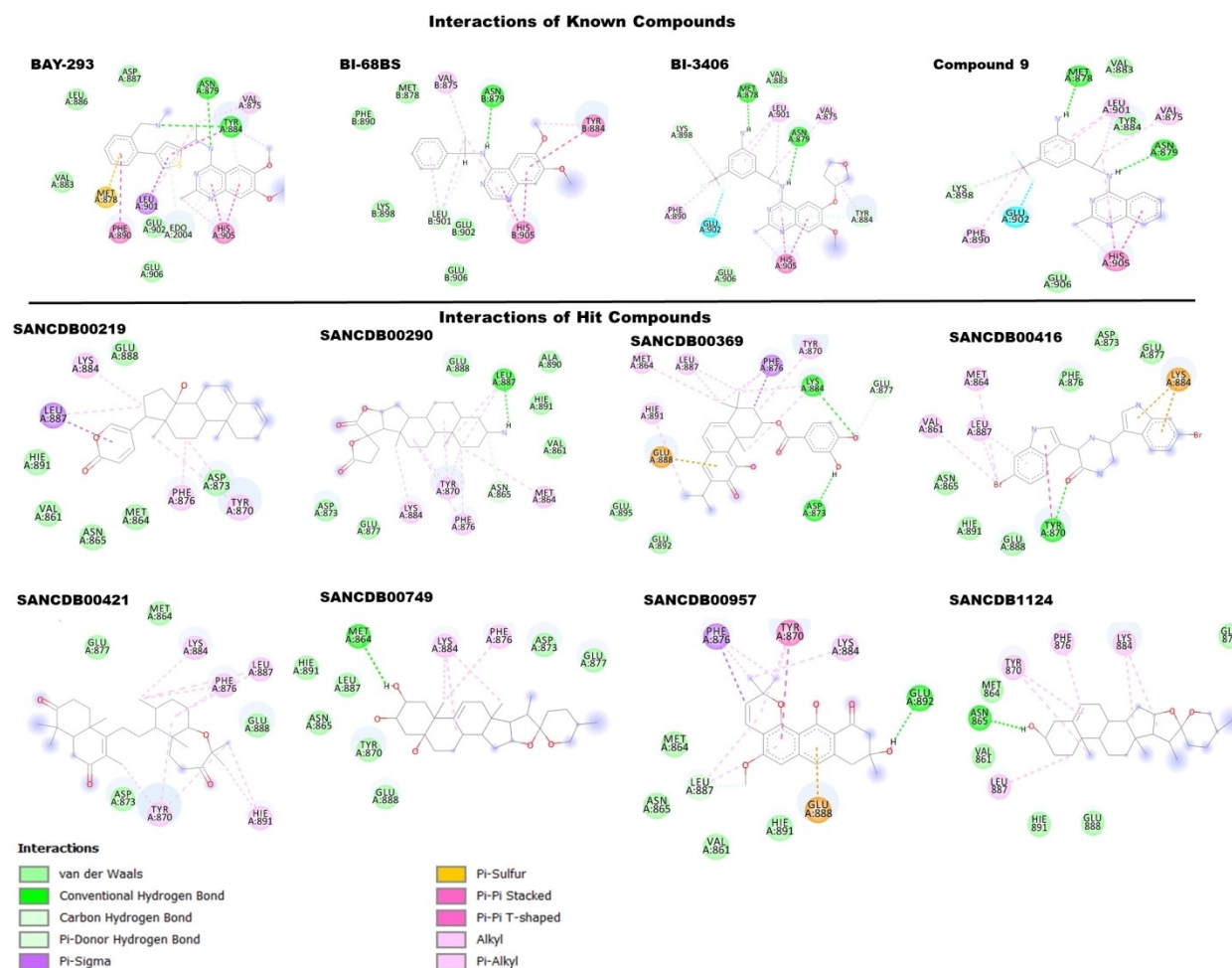
Figure 2. (A) 2D molecular interactions of known inhibitors within the binding site of the SOS1-KRAS allosteric binding site and (B) 2D molecular interactions of the hit compounds within the binding pocket of the SOS1-KRAS allosteric binding site.

Table 2. Binding energy profile of hit compounds.					
System	Energy components (kcal/mole)				
	ΔE_{vdw}	ΔE_{ele}	ΔG_{gas}	ΔG_{sol}	ΔG_{bind}
SANCDB00219	-29.77 ± 5.09	-8.90 ± 4.87	-38.67 ± 6.03	16.42 ± 3.84	-36.32 ± 4.23
SANCDB00290	-29.94 ± 5.18	-131.76 ± 24.02	-161.71 ± 24.29	140.69 ± 23.38	-32.42 ± 4.67
SANCDB00369	-36.40 ± 3.55	-50.19 ± 7.53	-86.60 ± 7.27	44.51 ± 5.41	-42.09 ± 3.54
SANCDB00416	-33.53 ± 3.99	-166.36 ± 12.61	-199.89 ± 14.37	175.96 ± 12.83	-32.23 ± 4.54
SANCDB00421	-34.42 ± 3.34	-3.36 ± 5.23	-37.78 ± 5.97	10.53 ± 4.87	-30.25 ± 3.41
SANCDB00749	-33.11 ± 4.17	-16.52 ± 7.06	-49.63 ± 7.43	21.74 ± 4.53	-30.89 ± 4.56
SANCDB00957	-31.90 ± 3.38	-16.77 ± 9.82	-48.67 ± 10.41	25.44 ± 9.24	-32.21 ± 4.26
SANCDB1124	-34.85 ± 5.19	-7.68 ± 4.59	-42.53 ± 7.53	13.41 ± 2.9	-35.11 ± 5.98

extracted from the rhizomes of *Elephantorrhiza elephantina*. Its medical use is not yet ascertained.[44]

Pharmacokinetics and PASS analysis of hit compounds

Since most drug failures occur at the clinical stage due to undesired pharmacokinetics, the selected compounds were then subjected to ADME analysis. The effectiveness of natural compounds against a particular disease depends on their bioactivities and the pharmacokinetic properties. The absorption, distribution, metabolism excretion and toxicity (ADMET) of the selected compounds are presented in Table 3. These properties were analyzed in accordance with traditional drug-like laws at the early stage of drug development. Lipinski's rule of five (RO5) was therefore employed as the basis for the analysis and subsequent elimination of some compounds. According to this rule, a compound's drug-likeness and use as a likely orally active drug in humans depends on itsability to

Table 3. Predicted physicochemical properties and toxicities of selected compounds.

Physiochemical propertie	Hit compounds							
MW	219	290	369	416	421	749	957	1124
Chemical formula	C24H30O3	C24H35NO4	C27H30O6	C20H16Br2 N4O	C30H46O4	C27H42O5	C21H22O5	C27H42O3
Molecular weight (g/mol)	366.49	401.54	450.52	488.18	470.68	446.62	354.40	414.62
Number of heavy atoms	27	29	33	27	34	32	26	30
Number of aromatic heavy atoms	6	0	6	18	0	0	10	0
Number of rotatable bonds	1	0	4	2	3	0	1	0
Number of H-bond acceptors	3	5	6	2	4	5	5	3
Number of H-bond donors	1	1	3	4	0	3	2	1
TPSA (Å2)	50.44	78.62	104.06	72.71	60.44	79.15	75.99	38.69
Molar Refractivity	107.45	109.59	126.11	120.95	138.34	123.96	100.44	121.59
LogPO/W	4.28	3.47	4.07	3.45	5.38	3.37	3.17	5.02
Blood brain barrier permeability	Yes	No	No	Yes	No	No	Yes	Yes
GI absorption	High	High	High	High	High	High	High	High
Toxicity profile								
LD50 (mg/kg)	5	5000	5000	313	6400	8000	500	8000
Toxicity class	1	5	5	4	5	6	4	6

Table 4. Results of PASS ONLINE calculations for hit compounds.

Antineoplastic activity

Compound	Antineoplastic		Antineoplastic (non-small lung cancer)		Antineoplastic (lung cancer)		Antineoplastic (color-ectal cancer)		Antineoplastic (pan-creatic cancer)	
	Pa	Pi	Pa	Pi	Pa	Pi	Pa	Pi	Pa	Pi
Clionamine D	0.659	0.033	–	–	0.396	0.024	0.205	0.062	0.354	0.030
14β-Hydroxybufa-3,5,20,22-tetraenolide	0.804	0.011	0.233	0.048	0.661	0.007	0.407	0.021	–	–
Parviflorone F	0.456	0,085	–	–	0.299	0.040	0.123	0.111	–	–
Cis-3,4-dihydrohamacanthin b	–	–	0.190	0.093	–	–	–	–	0.224	0.142
Sodwanone R	0.917	0.005	–	–	0.387	0.025	0.685	0.006	–	–
9(11)-Dehydroagapanthagenin	0.847	0.007	0.222	0.056	0.593	0.009	0.456	0.016	0.570	0.004
Vismione B	0.867	0.005	–	–	0.216	0.063	0.208	0.061	–	–
Diosgenin	–	–	0.246	0.041	0.538	0.012	0.345	0.029	0.705	0.003

satisfy the following conditions: molecular weight (MW) $\leq$ 500 Daltons; logP $\leq$ 5; Hydrogen bond acceptors (HBAs) $\leq$ 10 and Hydrogen bond donors (HBDs) $\leq$ 5. All selected compounds were predicted to possess high gastrointestinal absorption and good permeability. Though compound SANCDB00290, SANCDB00369, SANCDB00429 and SANCDB00749 were predicted as lacking the ability to cross the blood brain barrier (BBB), they presented good antineoplastic activities from the PASS analysis suggesting optimization and modifications could improve efficacy. Moreover, the therapeutic potentials of these compounds are targeted at non-small cell lung cancer, pancreatic cancer, colorectal cancer, and lung cancer which does not need BBB permeation. A significant percentage of these cancer types have been reported to result due to active KRAS inability to revert to its inactive state which is controlled by SOS1-KRAS-KRAS. Toxicity prediction as displayed in Table 3 showed SANCDB00749 and SANCDB1124 are non-toxic when administered orally whiles SANCDB00290, SANCDB00369, SANCDB00421, SANCDB00416 and SANCDB00957 showed moderate toxicity. SANCDB00219 was predicted to be very toxic when administered orally. However, these compounds were all considered for further analyses with the hypothesis that modification and optimization could lead to less toxicity and tolerance. As presented in Table 4, the compounds all showed Pa greater Pi in more than one of the above-mentioned diseased environments. These results show the compounds possess antineoplastic potentials worth harvesting. Having ascertained the physicochemical and antineoplastic properties of the compounds, their impact on the conformational dynamics of SOS1-KRAS was determined through 200 ns molecular dynamics simulation.

Hit compounds' stability consequentially stabilizes SOS1 active binding site

Bioactive compounds at the site of a protein engage in interactions with the residues within the site thus influencing changes that consequentially result in an activation or inhibitory effect of the protein.[45,46] The nature of the interactions involved in turn influences the stability of the compounds within the pocket. This phenomenon has been exploited by drug developers to curtail certain diseases including cancer. Interactions that underscored the differential compounds impact on the binding site are presented inFigure 3. The effect of the interactions on the stability of the compounds and the resultant effect on the binding site stability was therefore investigated through computing the root-mean square deviation of the atoms and C-α atoms of the compounds and site
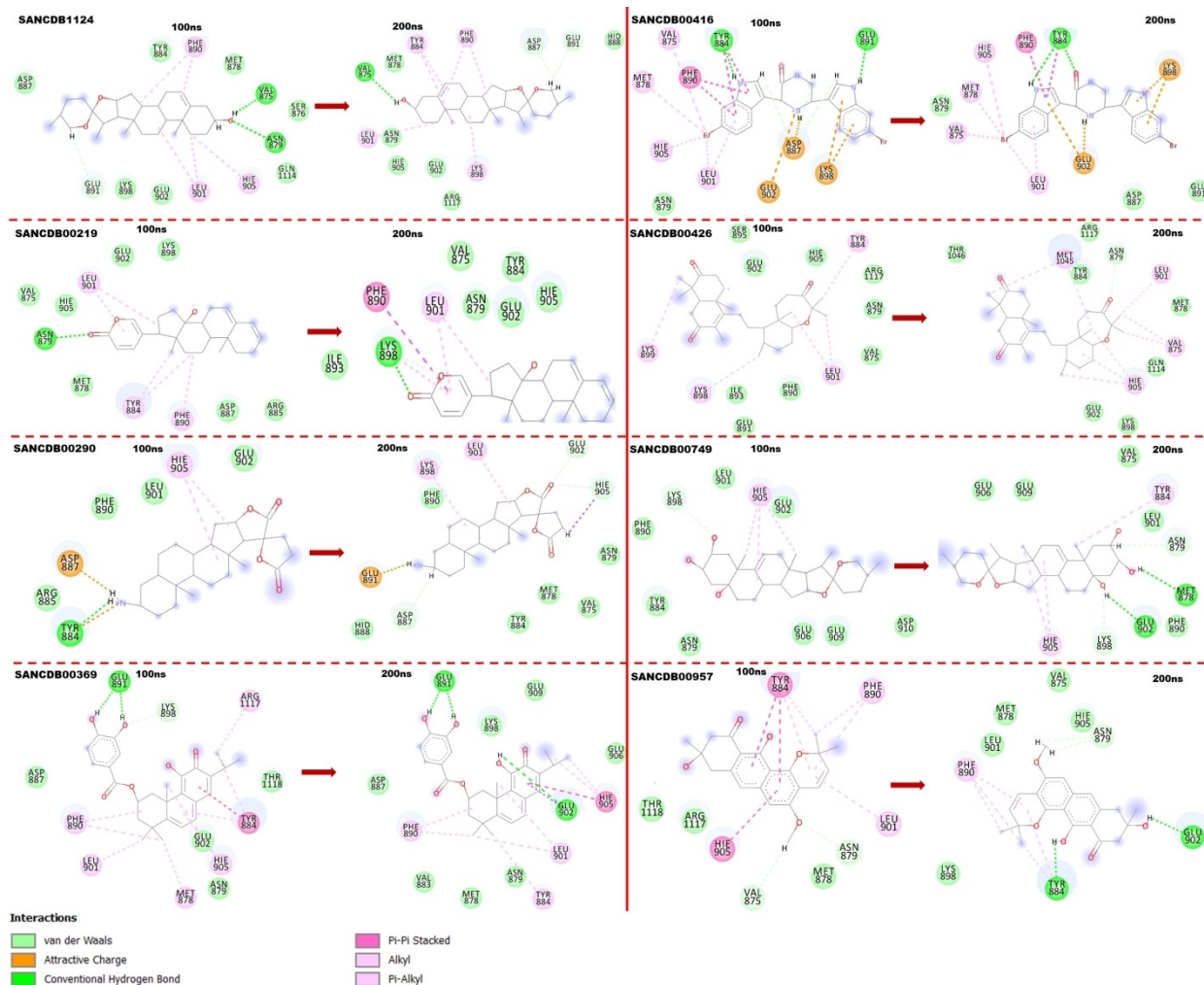
ChemistrySelect

Research Article
doi.org/10.1002/slct.202300277

Chemistry Europe
European Chemical
Societies Publishing

Figure 3. 2D interactions of hit compounds with SOS1 active binding site residues. Snapshots depicts interactions at 100 ns and 200 ns.

residues respectively. The results obtained indicate the eight compounds were stabilized throughout the 200 ns simulation time. Generally, the compounds exhibited average RMSD values below 2.0 Å. The three different resolutions of the protein showed a correlated trend; however, higher stability was observed among the protein with the higher resolution (7KFZ) and presented in the Figure 4. It was further observed that SANCDB00369 displayed the highest stability with an average RMD value of 0.47 Å. Investigation of the binding site showed that the compounds induced stability of the binding site. This was evidenced by the reduction in the deviations of the C-α atoms of the residues relative to the unbound protein and the global values (Supplementary Table S3, S4, S5, S6, S7, S8, S9 and S10). Average site values of 1.63 ± 0.20 Å, 1.77 ± 0.19 Å, 1.89 ± 0.26 Å, 1.58 ± 0.20 Å, 1.85 ± 0.17 Å, 1.80 ± 0.18 Å, 1.83 ± 0.17 Å, 1.72 ± 0.19 Å and 2.03 ± 0.22 Å were shown for SANCDB1124, SANCDB00219, SANCDB00290, SANCDB00369, SANCDB00416, SANCDB00421, SANCDB00749, SANCDB00957 occupied sites and the Apo, respectively. The binding site residues exhibited a general RMSD values below 2.0 Å compared to the apo and global protein values of 2.03 and

4.0 Å, respectively. The protein of the PDB ID 7KFZ was observed to present the most stable binding site. Again, SANCDB00369 induced the highest binding site stability.

Binding effect of hit compounds on protein-protein interaction interface of SOS1

The ultimate aim of SOS1-KRAS inhibition is the interjection of its activation of oncogenic KRAS. The activation occurs through the PPI interface where SOS1 engages KRAS.[47] Thus, the impact of the compounds on this interface is crucial in determining their therapeutic effects. As such, we determined the conformational changes that characterized the SOS1-KRAS interface. The stability (RMSD) and the surface area available for solvent interaction (SASA) was determined. This offers an insight into the folding/unfolding of the interface and repositioning of the interacting residues towards the hydrophilic/hydrophobic core of the binary proteins. As presented in Figure 5, the binding of the compounds induced a reduction in the C-α atoms deviations of the residues relative to the unbound (apo) protein. They presented average RMSD values
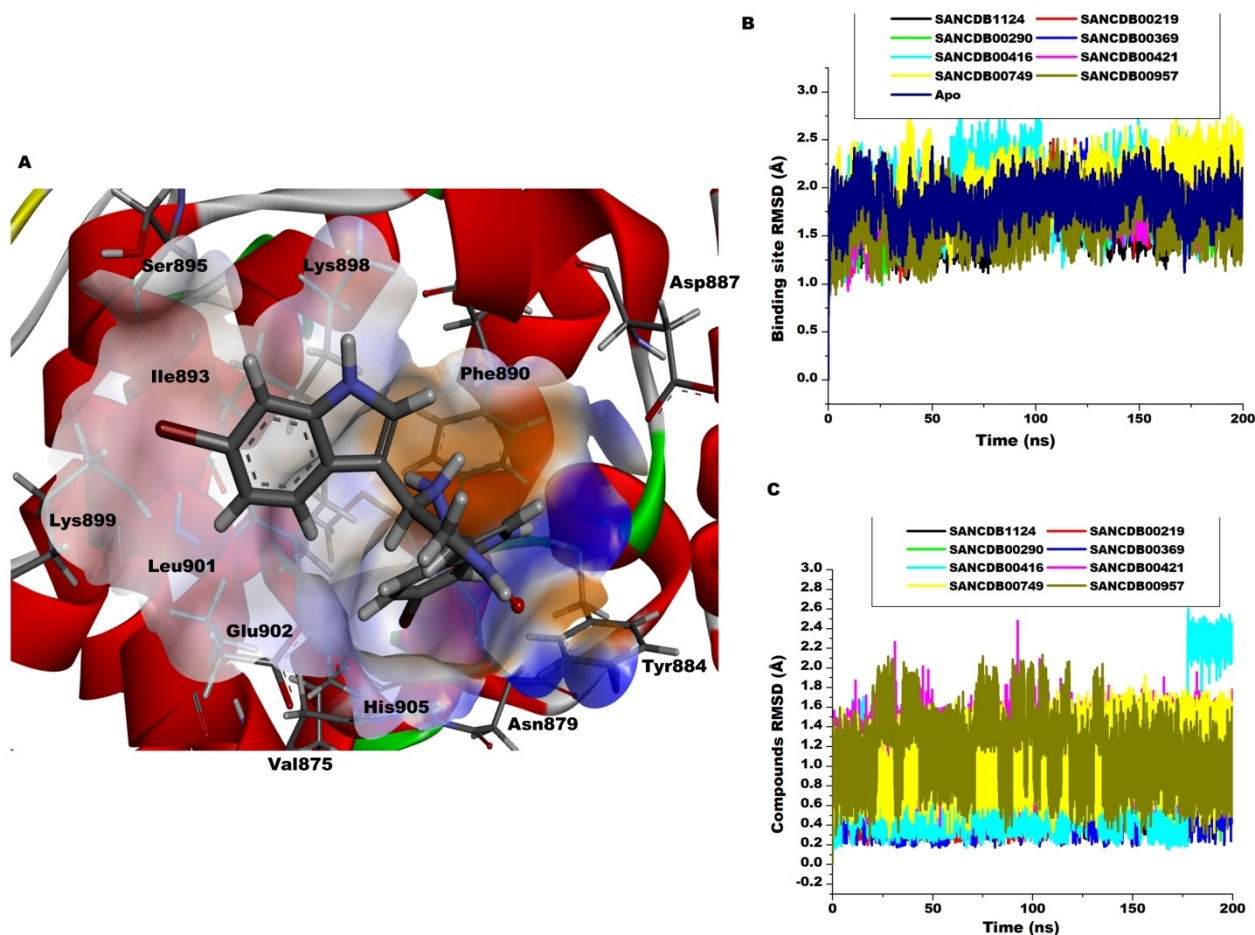
ChemistrySelect

Research Article
doi.org/10.1002/slct.202300277

Chemistry
Europe
European Chemical
Societies Publishing

Figure 4. Comparative stability of the compounds within the active binding site of SOS1 and their impact on the stability of the site residues. A) Shows the active binding site residues of SOS1 with a bound hit compound. B) Depicts the active binding site stability of SOS1 upon compounds' binding. C) Shows the stability of the compounds upon binding to SOS1 over the 200 ns simulation.

of 1.82±0.24, 1.91±0.20, 1.53±0.12, 1.70±0.16, 1.47±0.12, 2.09±0.16, 2.10±0.29, 1.56±0.15, and 2.14±0.15 for SANCDB1124, SANCDB00219, SANCDB00290, SANCDB00369, SANCDB00416, SANCDB00421, SANCDB00749, SANCDB00957 and Apo, respectively.

This effect corroborated with the solvent accessibility surface area, wherein the surface area of the residues accessible to the aqueous environment was reduced relative to the unbound protein. These further suggest the residues realigned towards the hydrophobic regions of the respective proteins thus reducing their contact which could resultantly sever the activation of oncogenic KRAS. Among the compounds, SANCDB00369 was observed to effect the most reduced SASA values.

Due to the distinguished effects of SANCDB00369 among the other compounds on the protein as observed in the investigations above, we further performed dynamic cross-correlation and principal component analysis on the SANCDB00369 complex.

SANCDB00369's bound complex shows correlated motions of switch I and II residues of KRAS

Probing further on the influence of SANCDB00369 on upon binding to the SOS1 active site, the variations in internal correlation motions relative to the unbound (Apo) protein was analyzed by cross-correlation matric of the C-α atom fluctuations. Figure 6 depicts the plots of the investigated regions and the binary complex proteins. Highly negative regions (blue-black) and highly positive regions (yellow-red) correlate with strong anti-correlated movements and strong correlated movements, respectively. Generally, the SANCDB00369 bound complex showed a more correlated motion among the residues of the switch I and switch II of KRAS. This is evidenced by the degree of positive regions (red) on the bound complex compared to the apo. A relatively lower correlated motions (cyan-yellow) was observed between residue 35–38 and residue 30–32 in switch I. Switch II also exhibited similar pattern of correlated intensity upon SANCDB00369 binding wherein relatively lower correlation (cyan-yellow) was observed between residues 63–78 and 58–62. Focusing on the global protein (SOS1-KRAS binary complex), the KRAS protein which
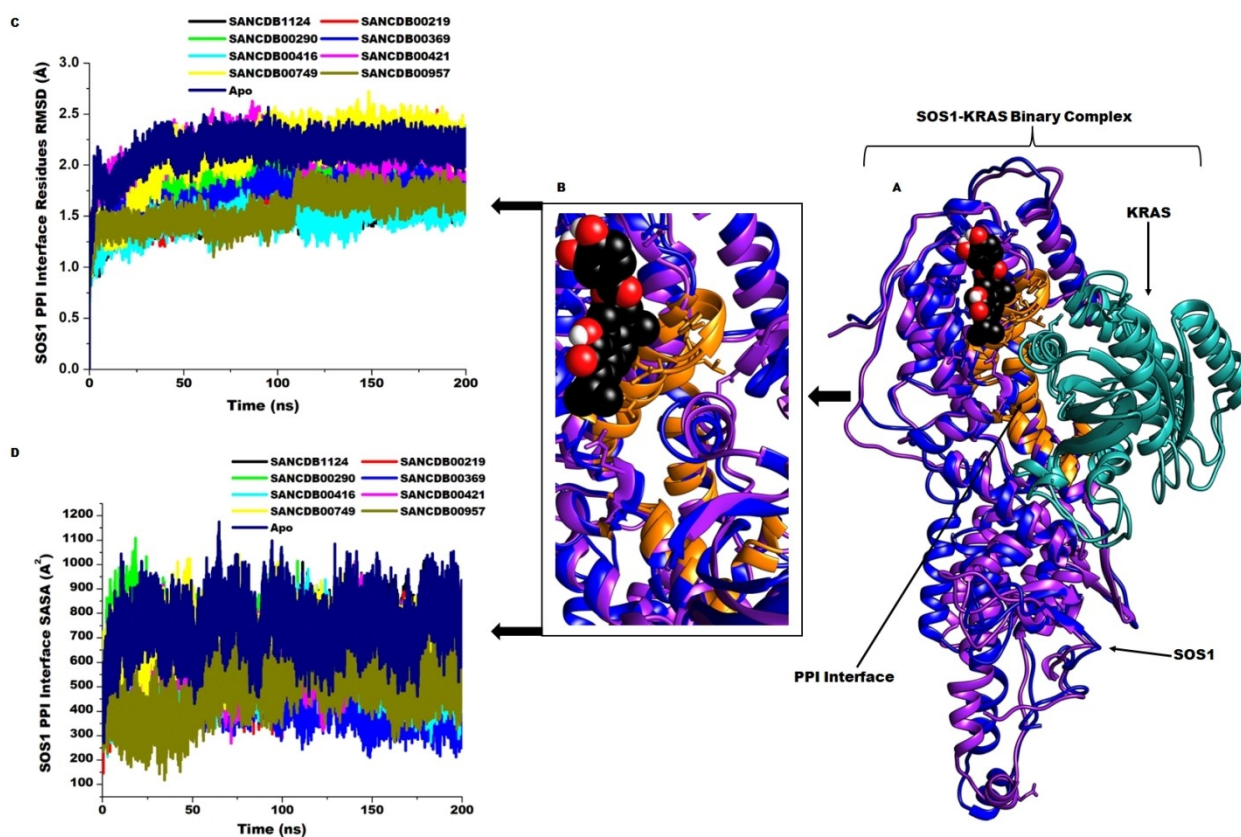
ChemistrySelect

Research Article
doi.org/10.1002/slct.202300277

Chemistry
Europe
European Chemical
Societies Publishing

Figure 5. Comparative plots of the impact of the hit compounds on the protein-protein interaction interface (PPI) between the SOS1 and KRAS. A) Superimposition of the binary complexes of the Apo (violet) and the SANCDB00369 bound (blue). Green indicates KRAS, while Orange shows the PPI interface. Black balls represent SANCDB00369. B) Shows zoning of the PPI interface. C) Shows the stability of the interface upon hits compounds binding over the period of simulation. D) Shows the solvent accessibility surface area (SASA) of the PPI over the simulation period.

corresponds to residues 480–647, exhibited the most positive correlated residues motions in the SANCDB00369 complex compared to the Apo. Also, the SANCDB00369 complex protein was further observed to display lesser correlation among the residues 1–180 compared to the Apo. Theses residues corresponds to the Ras Exchanger Motive (REM) domain of SOS1.[17] However, the CDC25 domain showed a similar correlation pattern among the bound and the apo (residues 180–479).

Further investigation into the conformational motions characterizing SANCD00369 and the Apo through principal component analysis (PCA) was performed. This matric offer considerable insights into the nature of the conformational changes that occur in protein structures during the simulation process in which large and concerted motions and underlying fluctuations are identified.[48,49] The main components of correlated motions of the structures were produced from covariance matrix diagonalization of the C-α atoms. The conformational behavior of SANCDB00369 bound complex and the Apo were therefore projected along the first two principal components or eigenvectors (ev1/PC1 vs ev2/PC2) directions.The projections are presented in Figure 7. The plots showed distinct conformational movements in the essential subspace along the two principal components. The bound proteins showed clear motion along the first principal

component compared to the Apo. The structure of a protein is related to its function thus changes in the structure and intricacies of a protein alters its function.[50,51] As such any influence on the structural and conformational dynamics of the binary protein complex beyond the native threshold by a small molecule could disrupt its functions. Thus, the observed differentials in the residues' movements in the bound and the unbound complexes could underscore the therapeutic potentials of the compounds.

Conformational dynamics of SOS1-KRAS binary complex upon compounds' binding

The binding of a bioactive compound to its target protein often induces conformational changes on the secondary and tertiary structure of the protein which results in influencing the basal functionalities of the protein.[52] These conformational and structural changes condition the therapeutic basis of the compounds. Thus, having ascertained the impact of these compounds at the regional levels, we further sought to determine their impact on the global proteins and the binary proteins. We first evaluated their stability and then the flexibility of the individual proteins through root mean square fluctuation (RMSF). As such, the computation of the RMSD and
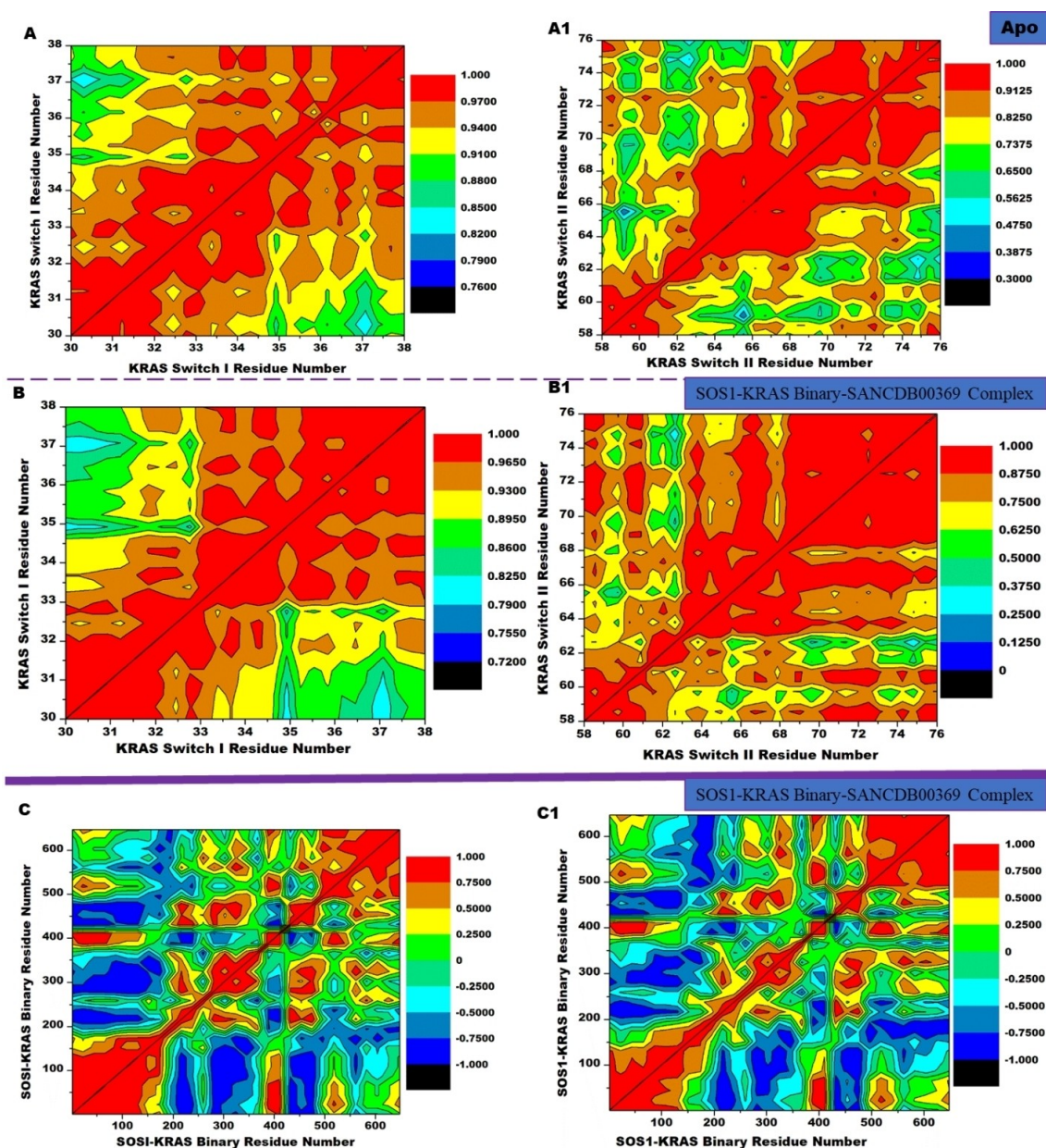
ChemistrySelect

Research Article
doi.org/10.1002/slct.202300277

**Chemistry
Europe**
European Chemical
Societies Publishing

Figure 6. Cross-correlation matrices of the fluctuations of coordinates of C-α atoms of the switches around their mean positions during 200 ns simulation. A and A1 show the cross-correlation of the switch I and switch II of the unbound protein (Apo), respectively. B and B2 show the cross-correlation of switch I and switch II of KRAS of the SOS1-KRAS binary complex upon SANCDB00369 binding, respectively. C and C1 show the global binary complex cross-correlation of the Apo and SANCDB00369 bound, respectively.

the RMSF of the C-α atoms of the SOS1-KRAS proteins upon the binding of the selected natural compounds revealed they induced a stable and less flexible protein. The estimation showed average RMSD values of 2.68 ± 0.23 Å, 2.79 ± 0.39 Å, 2.90 ± 0.33 Å, 3.13 ± 0.56 Å, 3.76 ± 0.63 Å, 3.63 ± 0.76 Å, 2.47 ± 0.44 Å, 2.52 ± 0.37 Å and 3.73 ± 0.57 Å for SANCDB00219, SANCDB00290, SANCDB00369, SANCDB00416, SANCDB00421, SANCDB00749, SANCDB00957, SANCDB1124 and the Apo, respectively. This matric which is informative on the stability of the proteins via the C-α atoms deviation from the initial starting structure through the period of simulation. As

observed in Figure 8, all the natural compounds except SANCDB00421 (3.76 Å) induced a more stable SOS1-KRAS protein compared to the Apo (unbound) while SANCDB00957 was observed to induce the most stable protein. The overall presentation of the RMSD matric of the system is also indicative of system convergence during the period of simulation. Further, the RMSF of the C-α atoms also presented 10.46 ± 4.11 Å, 11.36 ± 4.28 Å, 9.15 ± 3.45 Å, 11.43 ± 4.25 Å, 11.51 ± 3.96 Å, 9.98 ± 4.05 Å, 10.41 ± 3.7 Å, 12.59 ± 4.9 Å and 14.10 ± 6.12 Å as average values for SANCDB00219, SANCDB00290, SANCDB00369, SANCDB416, SANCDB421, SANCDB00957,

ChemistrySelect

Research Article
doi.org/10.1002/slct.202300277

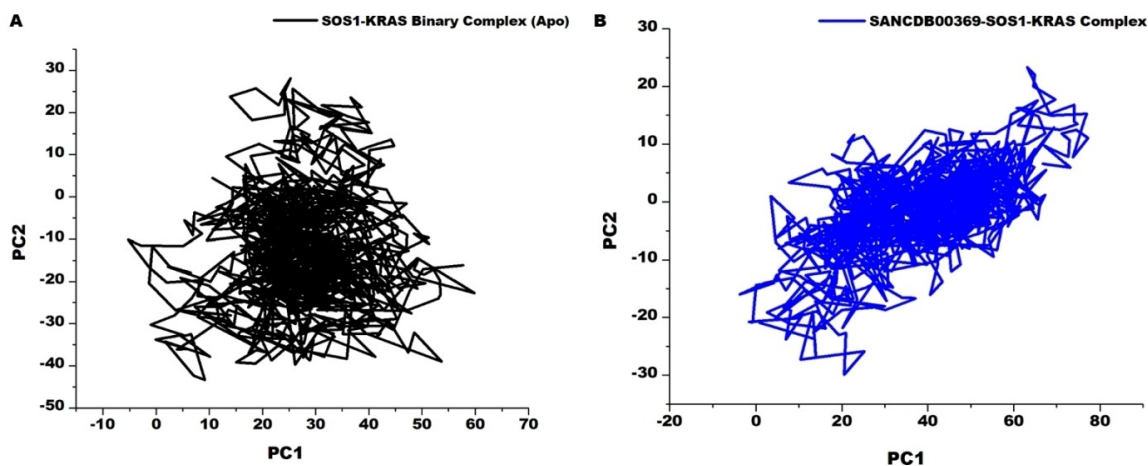**Chemistry Europe**
European Chemical
Societies Publishing

Figure 7. PCA projections of C-α atoms motions of the Apo and SANCDB00369 constructed by plotting the first two principal components (PC1 and PC2) in conformational subspace. A) Shows the construct of the residual fluctuations of the unbound (Apo) binary complex. B) Shows the construct of the residual fluctuations of the SANCDB00369 complex.
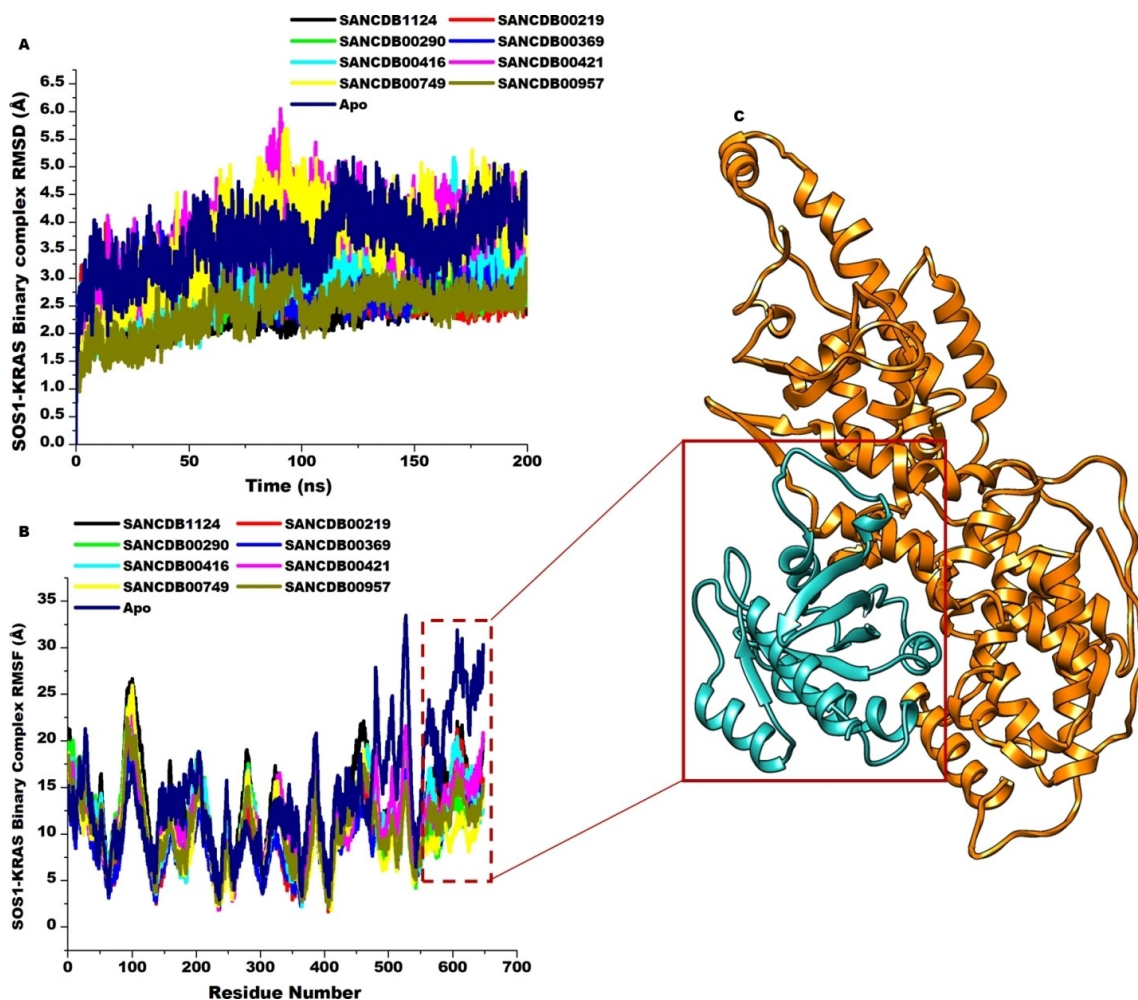

Figure 8. Comparative C-α RMSD and RMSF plots showing the degree of stability and individual residue fluctuation of the SOS1-KRAS protein upon binding of the hit compounds. **A)** Shows the RMSD plots of the SOS1-KRAS which indicate the compounds induced relative stability of the SOS1-KRAS protein upon binding. **B)**. Shows the RMSF plots indicating all compounds binding the residual fluctuations of the KRAS protein. C) Insert highlights the reduction in KRAS fluctuation compared to the Apo.

SANCDB1124 and the Apo, respectively. As observed, all the compounds bound proteins presented lower values compared to the unbound SOS1-KRAS. The general lower results of the compounds indicate the compounds upon binding reduce the conformational flexibility of the SOS1-KRAS protein. The reduction in flexibility could result in severing the interaction between the SOS1 protein and the KRAS protein via the folding of the interaction interface, hence moderating their therapeutic prowess.

Conclusion

Traditionally, natural compounds have been a source of therapeutic agents for the treatment of a wide variety of diseases such as cancer. In this research, we utilized the South African natural compounds database and computational tools to identify natural compounds with inhibitory potentials against SOS1-KRAS interactions. After screening 1,132 natural compounds, 58 compounds were initially selected *via* their docking scores. Subsequent analysis of the compounds through ADMET and PASS online activity assessment finally led to the selection of 8 compounds with good pharmacokinetics and antineoplastic activities. These eight compounds were then subjected to 200 ns molecular dynamics simulation, and their total free binding energies calculated over 10,000 snapshots. The compounds showed favorable total free binding energies indicative of their spontaneity in complexing with the SOS1-KRAS protein. Further analysis on the global impact of the compounds on the SOS1-KRAS protein showed the compounds induced a stable SOS1-KRAS protein with reduced flexibility of the C-α atoms. These findings suggest the compounds could be considered as potential drug-like compounds in the inhibition of SOS1-KRAS interactions. The biological potential of these compounds could further be confirmed through experimental studies. This study will therefore be useful in the design of specific drugs for therapeutic inhibition of SOS1-KRAS.

Supporting Information Summary

This section contains the Materials and methods Section, Figure S1 and Tables (Table S1 to S10).**Figure S1**. Graphs showing the validation of SOS1-KRAS protein structures used for docking and MD simulation. A and A1 show the Ramachandran plot and the overall QMEAN4 global quality graph of 7KFZ respectively. B and B1 show the Ramachandran plot and the overall QMEAN4 global quality graph of 6EPP respectively and, C and C1 show the Ramachandran plot and the overall QMEAN4 global quality graph of 6EPN, respectively.**Table S1**. First selected compounds from structure-based virtual screening, **Table S2**. Docking results for known inhibitors, **Table S3**. GLOBAL (SOS1-KRAS binary complex) RMSD (Å) data, **Table S4**. Global (SOS1-KRAS binary complex) RMSF (Å) data, **Table S5**. Ligand (Hit compound) RMSD (Å) data, **Table S6**. SOS1 binding site RMSD (Å) data, **Table S7**.KRAS RMSD (Å) data, **Table S8**. KRAS RMSF (Å) data, **Table S9**. SOS1 RMSD (Å) data, **Table S10**.

SOS RMSF (Å) data. Additional references cited within the Supporting Information.[53–88]

Conflict of Interests

There is no conflict of interest with other people or organizations that could inappropriately influence or bias the content of the paper.

Data Availability Statement

The data that support the findings of this study are available in the supplementary material of this article.

[1] A. D. Cox, S. W. Fesik, A. C. Kimmelman, J. Luo, C. J. Der, *Nat. Rev. Drug Discovery* **2014**, *13*, 828–851.
[2] G. A. Hobbs, C. J. Der, K. L. Rossman, *J. Cell Sci.* **2016**, *129*, 1287–1292.
[3] D. K. Simanshu, D. V. Nissley, F. McCormick, *Cell* **2017**, *170*, 17–33. doi:10.1016/j.cell.2017.06.009.
[4] E. Santos, A. R. Nebreda, *FASEB J.* **1989**, *3*, 2151–2163.
[5] R. C. Hillig, B. Sautier, J. Schroeder, D. Moosmayer, A. Hilpmann, C. M. Stegmann, N. D. Werbeck, H. Briem, U. Boemer, J. Weiske, V. Badock, J. Mastouri, K. Petersen, G. Siemeister, J. D. Kahmann, D. Wegener, N. Böhnke, K. Eis, K. Graham, L. Wortmann, F. von Nussbaum, B. Bader, *Proc. Natl. Acad. Sci. USA* **2019**, *116*, 2551–2560.
[6] K. M. Haigis, *Trends Cancer* **2017**, *3*, 686–697.
[7] J. Downward, *Nat. Rev. Cancer* **2003**, *3*, 11–22.
[8] J. M. L. Ostrem, K. M. Shokat, *Nat. Rev. Drug Discovery* **2016**, *15*, 771–785.
[9] A. Indini, E. Rijavec, M. Ghidini, A. Cortellini, F. Grossi, *Pharmaceutica* **2021**, *13*, 1–17.
[10] J. Canon, K. Rex, A. Y. Saiki, C. Mohr, K. Cooke, D. Bagal, K. Gaida, T. Holt, C. G. Knutson, N. Koppada, B. A. Lanman, J. Werner, A. S. Rapaport, T. San Miguel, R. Ortiz, T. Osgood, J. R. Sun, X. Zhu, J. D. McCarter, L. P. Volak, B. E. Houk, M. G. Fakih, B. H. O'Neil, T. J. Price, G. S. Falchook, J. Desai, J. Kuo, R. Govindan, D. S. Hong, W. Ouyang, H. Henary, T. Arvedson, V. J. Cee, J. R. Lipford, *Nature* **2019**, *575*, 217–223.
[11] M. Xie, X. Xu, Y. Fan, *Front. Oncol.* **2021**, *11*, 672612.
[12] H. Chen, J. B. Smaill, T. Liu, K. Ding, X. Lu, *J. Med. Chem.* **2023**, *63*, 14404–14424.
[13] M. R. Janes, J. Zhang, L.-S. Li, R. Hansen, U. Peters, X. Guo, Y. Chen, A. Babbar, S. J. Firdaus, L. Darjania, J. Feng, J. H. Chen, S. Li, S. Li, Y. O. Long, C. Thach, Y. Liu, A. Zarieh, T. Ely, J. M. Kucharski, L. V. Kessler, T. Wu, K. Yu, Y. Wang, Y. Yao, X. Deng, P. P. Zarrinkar, D. Brehmer, D. Dhanak, M. V. Lorenzi, D. Hu-Lowe, M. P. Patricelli, P. Ren, Y. Liu, *Cell* **2018**, *172*, 578–589 e17.
[14] M. P. Patricelli, M. R. Janes, L.-S. Li, R. Hansen, U. Peters, L. V. Kessler, Y. Chen, J. M. Kucharski, J. Feng, T. Ely, J. H. Chen, S. J. Firdaus, A. Babbar, P. Ren, Y. Liu, *Cancer Dis.* **2016**, *6*, 316–329.

[15] T. Li, R. Wernersson, R. B. Hansen, H. Horn, J. Mercer, G. Slodkowicz, C. T. Workman, O. Rigina, K. Rapacki, H. H. Stærfeldt, S. Brunak, T. S. Jensen, K. Lage, *Nat. Methods* **2017**, *14*, 61–64.

[16] P. A. Boriack-Sjodin, S. M. Margarit, D. Bar-Sagi, J. Kuriyan, *Nature* **1998**, *394*, 337–343.

[17] T. S. Freedman, H. Sondermann, G. D. Friedland, T. Kortemme, D. Bar-Sagi, S. Marqusee, J. Kuriyan, *Proc. Natl. Acad. Sci. USA* **2006**, *103*, 16692–16697.

[18] D. Vigil, J. Cherfils, K. L. Rossman, C. J. Der, *Nat. Rev. Cancer* **2010**, *10*, 842–857.

[19] E. Sheffels, N. E. Sealover, C. Wang, D. H. Kim, I. A. Vazirani, E. Lee, M. E. Terrell, D. K. Morrison, J. Luo, R. L. Kortum, *Sci. Signaling* **2018**, *11*, eaar8371.

[20] J. J. G. Winter, M. Anderson, K. Blades, C. Brassington, A. L. Breeze, C. Chresta, K. Embrey, G. Fairley, P. Faulder, M. R. V. Finlay, J. G. Kettle, T. Nowak, R. Overman, S. J. Patel, P. Perkins, L. Spadola, J. Tart, J. A. Tucker, G. Wrigley, *J. Med. Chem.* **2015**, *58*, 2265–2274.

[21] C. R. Evelyn, X. Duan, J. Biesiada, W. L. Seibel, J. Meller, Y. Zheng, *Chem. Biol.* **2014**, *21*, 1618–1628.

[22] M. C. Burns, J. E. Howes, Q. Sun, A. J. Little, D. V. Camper, J. R. Abbott, J. Phan, T. Lee, A. G. Waterson, O. W. Rossanese, S. W. Fesik, *Anal. Biochem.* **2018**, *548*, 44–52.

[23] M. C. Burns, Q. Sun, R. N. Daniels, D. Camper, J. P. Kennedy, J. Phan, E. T. Olejniczak, T. Lee, A. G. Waterson, O. W. Rossanese, S. W. Fesik, *Proc. Natl. Acad. Sci. USA* **2014**, *111*, 3401–3406.

[24] J. E. Howes, D. T. Akan, M. C. Burns, O. W. Rossanese, A. G. Waterson, S. W. Fesik, *Mol. Cancer Ther.* **2018**, *17*, 1051–1060.

[25] A. B. Deore, J. R. Dhumane, R. Wagh, R. Sonawane, *Asian J. Pharm.* **2019**, *7*, 62–67.

[26] J. P. Hughes, S. Rees, S. B. Kalindjian, K. L. Philpott, *Br. J. Pharmacol.* **2011**, *162*, 1239–1249.

[27] R. C. Mohs, N. H. Greig, *Alzheimer's Dementia* **2017**, *3*, 651–657.

[28] S. Pushpakom, F. Iorio, P. A. Eyers, K. J. Escott, S. Hopper, A. Wells, A. Doig, T. Guilliams, J. Latimer, C. McNamee, A. Norris, P. Sanseau, D. Cavalla, M. Pirmohamed, *Nat. Rev. Drug Discovery* **2019**, *18*, 41–58.

[29] N. C. Baker, S. Ekins, A. J. Williams, A. Tropsha, *Drug Discovery Today* **2018**, *23*, 661–672.

[30] C. Veeresham, *J. Adv. Pharm. Technol. Res.* **2012**, *3*, 200–201.

[31] G. Rastelli, F. Pellati, L. Pinzi, M. C. Gamberini, *Molecules* **2020**, *25*, 1154.

[32] D. J. Newman, G. M. Cragg, *J. Nat. Prod.* **2016**, *79*, 629–661.

[33] B. L. DeCorte, *J. Med. Chem.* **2016**, *59*, 9295–9304.

[34] M. Dell'Agli, F. Giavarini, P. Ferraboschi, G. Galli, E. Bosisio, *J. Agric. Food Chem.* **2007**, *55*, 3363–3367.

[35] J. D. Durrant, J. A. McCammon, *BMC Biol.* **2011**, *9*, 71.

[36] A. R. Issahaku, A. Aljoundi, M. E. S. Soliman, *Informatics Med. Unlocked* **2022**, *30*, 100952.

[37] F. Fusi, A. Ferrara, C. Koorbanally, N. R. Crouch, D. A. Mulholland, G. Sgaragli, *J. Pharm. Pharmacol.* **2008**, *60*, 489–497.

[38] N. A. Koorbanally, C. Koorbanally, A. Harilal, D. A. Mulholland, N. R. Crouch, *Phytochemistry* **2004**, *65*, 3069–3073.

[39] R. A. Keyzers, J. Daoust, M. T. Davies-Coleman, M. T. R. V. Soest, A. Balgi, E. Donohue, M. Roberge, R. J. Andersen, *Org. Lett.* **2008**, *10*, 2959–2962.

[40] R. L. Van Zyl, F. Khan, T. J. Edwards, S. E. Drewes, *South Afr. J. Sci.* **2008**, *104*, 62–64.

[41] R. Zoraghi, L. Worrall, R. H. See, W. Strangman, W. L. Popplewell, H. Gong, T. Samaai, R. D. Swayze, S. Kaur, M. Vuckovic, B. B. Finlay, R. C. Brunham, W. R. McMaster, M. T. Davies-Coleman, N. C. Strynadka, R. J. Andersen, N. E. Reiner, *J. Biol. Chem.* **2011**, *286*, 44716–44725.

[42] A. Rudi, T. Yosief, M. Schleyer, Y. Kashman, *Tetrahedron* **1999**, *55*, 5555–5566.

[43] A. G. González, C. G. Francisco, R. Freire, R. Hernández, J. A. Salazar, E. Suárez, *Phytochemistry* **1975**, *14*, 2259–2262.

[44] C. Raudsepp-Hearne, A. Aiello, A. A. Hussein, M. V. Heller, T. Johns, T. L. Capson, *J. Chem. Ecol.* **2015**, *41*, 816–821.

[45] S. J. Mpofu, T. A. M. Msagati, R. W. M. Krause, *Afr. J. Tradit. Complementary Altern. Med.* **2014**, *11*, 34–52.

[46] A. R. Issahaku, C. Agoni, O. S. Soremekun, P. A. Kubi, R. K. Oduro, F. A. Olotu, M. E. S. Soliman, *Comb. Chem. High Throughput Screening* **2019**, *22*, 521–533.

[47] A. R. Issahaku, N. Mukelabai, C. Agoni, M. Rudrapal, S. M. Aldosari, S. G. Almalki, J. Khan, *Sci. Rep.* **2022**, *12*, 17796.

[48] D. J. Bartholomew, Principal components analysis, in *International Encyclopedia of Education*, R. Tierney, F. Rizvi, K. Ercikan, eds., Elsevier, USA, **2022**, 54–57.

[49] A. M. Martinez, A. C. Kak, *Trans. Pattern Anal. Mach. Intell.* **2001**, *23*, 228–233.

[50] I. N. Berezovsky, E. Guarnera, Z. Zheng, *Prog. Biophys. Mol. Biol.* **2017**, *128*, 85–99.

[51] A. Amadei, A. B. M. Linssen, H. J. C. Proteins, *Struct. Funct. Bioinform.* **1993**, *17*, 412–425.

[52] I. Rehman, M. Farooq, S. Botelho, *Biochemistry, Secondary Protein Structure*, StatPearls, Internet, **2021**.

[53] B. N. Diallo, M. Glenister, T. M. Musyoka, K. Lobb, K. Ö Tastan Bishop, *J. Cheminf.* **2021**, *13*, 37.

[54] R. Hatherley, D. K. Brown, T. M. Musyoka, D. L. Penkler, N. Faya, K. A. Lobb, Ö. Tastan Bishop, *J. Cheminf.* **2015**, *7*, 29.

[55] Z. Moghadamchargari, M. Shirzadeh, C. Liu, S. Schrecke, C. Packianathan, D. H. Russell, M. Zhao, A. Laganowsky, *Proc. Natl. Acad. Sci. USA* **2021**, *118*, e2022403118.

[56] H. M. Berman, J. Westbrook, Z. Feng, G. Gilliland, T. N. Bhat, H. Weissig, I. N. Shindyalov, P. E. Bourne, *Nucleic Acids Res.* **2000**, *28*, 235.

[57] J. J. G. Winter, M. Anderson, K. Blades, C. Brassington, A. L. Breeze, C. Chresta, K. Embrey, G. Fairley, P. Faulder, M. R. Finlay, P. Faulder, M. R. V. Finlay, J. G. Kettle, *J. Med. Chem.* **2015**, *58*, 2265–2274.

[58] E. F. Pettersen, T. D. Goddard, C. C. Huang, G. S. Couch, D. M. Greenblatt, E. C. Meng, T. E. Ferrin, *J. Comput. Chem.* **2004**, *25*, 1605–1612.

[59] N. Eswar, B. Webb, M. A. Marti-Renom, M. S. Madhusudhan, D. Eramian, M.-Y. Shen, U. Pieper, A. Sali, *Comparative protein structure modeling using Modeller*, Curr. Protoc. Bioinforma. Chapter5(**2006**), Unit-5.6. doi:10.1002/0471250953.bi0506 s15.

[60] *ZLab*, Available online: https://www.umassmed.edu/zlab/ (accessed on Dec 20, 2021).

[61] P. Benkert, M. Biasini, T. Schwede, *Bioinformatics* **2011**, *27*, 343–350.

[62] T. Schwede, J. Kopp, N. Guex, M. C. Peitsch, *Nucleic Acids Res.* **2003**, *31*, 3381–3385.

[63] M. Wiederstein, M. J. Sippl, *Nucleic Acids Res.* **2007**, *35*, W407–W410.

[64] N. M. O'Boyle, M. Banck, C. A. James, C. Morley, T. Vandermeersch, G. R. Hutchison, *J. Cheminf.* **2011**, *3*, 33.

[65] M. H. Hofmann, J. Gmachl, J. Ramharter, F. Savarese, D. Gerlach, J. R. Marszalek, M. P. Sanderson, D. Kessler, F. Trapani, H. Arnhof, K. Rumpel, *Cancer Dis.* **2021**, *11*, 142–157.

[66] J. Ramharter, D. Kessler, P. Ettmayer, M. H. Hofmann, T. Gerstberger, M. Gmachl, T. Wunberg, C. Kofink, M. Sanderson, H. Arnhof, G. Bader, *J. Med. Chem.* **2021**, *64*, 6569–6580.

[67] P. Banerjee, A. O. Eckert, A. K. Schrey, R. Preissner, *Nucleic Acids Res.* **2018**, *46*, W257–W263.

[68] P. Banerjee, F. O. Dehnbostel, R. Preissner, *Front. Chem.* **2018**, *6*, 362.

[69] M. N. Drwal, P. Banerjee, M. Dunkel, M. R. Wettig, R. Preissner, *Nucleic Acids Res.* **2014**, *42*, 53–58.

[70] A. Daina, O. Michielin, V. Zoete, *Sci. Rep.* **2017**, *7*, 1–13.

[71] *Computational tools for ADMET*, Available online: http://crdd.osdd.net/admet.php (accessed on Dec 8, 2021).

[72] D. Filimonov, V. Poroikov, *Chemoinformatics Approaches to Virtual Screen* **2009**, 182–216.

[73] A. Lagunin, A. Stepanchikova, D. Filimonov, V. Poroikov, *Bioinformatics* **2000**, *16*, 747–748.

[74] D. S. Jairajpuri, A. Hussain, K. Nasreen, T. Mohammad, F. Anjum, M. R. Tabish, G. H. Mustafa, M. F. Alajmi, M. H. Imtaiyaz, *Saudi J. Biol. Sci.* **2021**, *28*, 2423–2431.

[75] D. A. Case, V. Babin, J. Berryman, R. M. Betz, Q. Cai, D. S. Cerutti, T. E. Cheatham III, T. A. Darden, R. E. Duke, H. Gohlke, *Amber* **2018**, *2018*, .

[76] K. G. Sprenger, V. W. Jaeger, J. Pfaendtner, *J. Phys. Chem. B* **2015**, *119*, 5882–5895.

[77] J. A. Maier, C. Martinez, K. Kasavajhala, L. Wickstrom, K. E. Hauser, C. J. Chem. Theory Comput. **2015**, *11*, 3696–3713.

[78] S. Nikitin, *Leap Gradient Algorithm*, **2014**.

[79] P. Gonnet, *J. Comput. Phys.* **2007**, *220*, 740–750.

[80] A. R. Issahaku, M. E. S. Soliman, *Curr. Pharm. Biotechnol.* **2022**.

[81] A. R. Issahaku, E. Y. Salifu, M. E. S. Soliman, *J. Biomol. Struct. Dyn.* **2022**, 1–13.

[82] K. A. Agha, N. E. Abo-Dya, A. R. Issahaku, C. Agoni, M. E. S. Soliman, E. H. Abdel-Aal, Z. K. Abdel-Samii, T. S. Ibrahim, *J. Enzyme Inhib. Med. Chem.* **2022**, *37*, 1241–1256.

[83] M. Rudrapal, A. R. Issahaku, C. Agoni, A. R. Bendale, A. Nagar, M. E. S. Soliman, D. Lokwani, *J. Biomol. Struct. Dyn.* **2022**, *40*, 10437–10453.

[84] D. R. Roe, T. E. Cheatham, *J. Chem. Theory Comput.* **2013**, *9*, 3084–3095.

[85] D. S. BIOVIA, Discovery Studio 2017, **2017**.

[86] E. Seifert, *J. Chem. Inf. Model.* **2014**, *54*, 1552.

[87] B. R. Miller, T. D. J. McGee, J. M. Swails, N. Homeyer, H. Gohlke, A. E. Roitberg, *J. Chem. Theory Comput.* **2012**, *8*, 3314–3321.

[88] V. P. Archana, S. J. Armaković, S. Armaković, I. Celik, J. B. Bhagyasree, K. D. Babu, M. Rudrapal, I. S. Divya, R. R. Pillai, *J. Mol. Struct.* **2023**, *1281*, 135110.